# A Remarkable Skeletal Rearrangement of a Coordinated Tetrapyrrole: Chemical Consequences of Palladium $\pi$-Coordination to a Bilindione

**Pamela A. Lord,[‡] Bruce C. Noll,[§] Marilyn M. Olmstead,[‡] and Alan L. Balch*[,‡]**

*Contribution from the Department of Chemistry, University of California, Davis, California 95616, and the Department of Chemistry and Biochemistry, University of Colorado, Boulder, Colorado 80309*

*Received March 12, 2001. Revised Manuscript Received July 6, 2001*

**Abstract:** $Pd_4(OEB)_2$, in which a $[Pd_2]^{2+}$ unit is bound in $\pi$-fashion to olefinic sites that are exocyclic to pyrrole rings of the octaethylbilindione ligand, undergoes an unprecedented sequence of reactions that results in the rearrangement of the framework of the bilindione ligand and the formation of *trans*-$Pd(py)_2I_2$. This process of bilindione rearrangement and oxidation occurs as a direct consequence of the $\pi$-coordination of the palladium. The reaction results in the migration of a nitrogen atom from a pyrrole carbon atom to what was formerly a meso carbon atom to transform a former pyrrole ring into a six-membered ring. This process also involves cleavage of the Pd−Pd and Pd−C bonds, oxidation of palladium, and introduction of an oxygen atom (from water) not necessarily in this particular sequence.

## Introduction

The bile pigment biliverdin IX$\alpha$, a bilindione whose structure is shown in part A of Chart 1, is formed by oxidative attack upon the $\alpha$-methine position of heme by the enzyme heme oxygenase.[1,2] During this process an iron complex of biliverdin is an intermediate, but the details of the axial ligation, oxidation state, and spin state are not available. However, studies of the model compound octaethylbilindione ($H_3$OEB, see Chart 1), show that the iron complex undergoes ready dissociation into free iron and free ligand.[3] Other metal ions including Cu(II),[4] Ni(II),[5,6] and Co(II)[7−9] form stable complexes with octaethylbilindione. These complexes show remarkable redox activity as a part of the three-membered, electron-transfer series shown in part B of Chart 1. On the other hand Mn(III) and Fe(III) bind to octaethylbilindione to form binuclear complexes as shown in part C of Chart 1.[3,7] Biliverdin IX$\alpha$ has been found to have both anti-oxidant activity[10] and anti-HIV activity.[11,12] Biliverdin is also widely utilized as a pigment by various organisms.[13] For example, zinc biliverdin is found in birds' eggs.

**Chart 1**

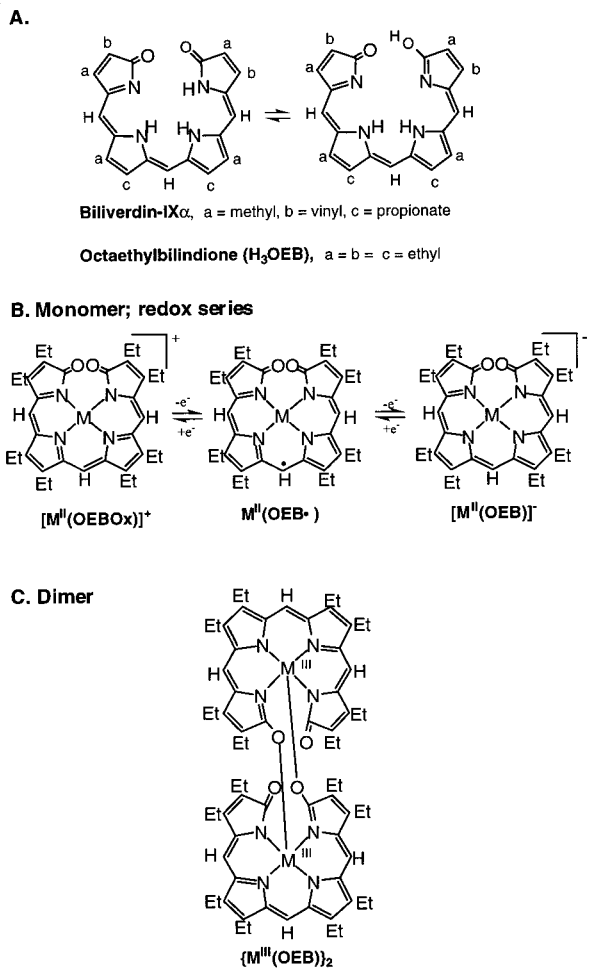


Recent work has revealed the ability of tetrapyrrole ligands, including porphyrins, porphyrinogens, and bilindiones, to coordinate metal ions in a $\pi$-fashion as well as in the usual $\sigma$-fashion through the nitrogen lone pairs.[14] Some relevant examples of such $\pi$-coordination include a sandwich structure with two lithium ions surrounded by two ruthenium(OEP)

[‡] University of California.
[§] University of Colorado.

(1) Maines, M. D. *Heme Oxygenase: Clinical Applications and Functions;* CRC Press: Boca Raton, FL, 1992.
(2) Ortiz de Montellano, P. R.; Wilks, A. *Adv. Inorg. Chem.* **2001**, *51*, 359.
(3) Balch, A. L.; Latos-Graożyński, L.; Noll, B. C.; Olmstead, M. M.; Safari, N. *J. Am. Chem. Soc.* **1993**, *115*, 9056.
(4) Balch, A. L.; Mazzanti, M.; Noll, B. C.; Olmstead, M. M. *J. Am. Chem. Soc.* **1993**, *115*, 12206.
(5) Bonfiglio, J. V.; Bonnett, R.; Buckley, D. G.; Hamzetash, D.; Hursthouse, M. B.; Abdul Malik, K. M.; McDonagh, A. F.; Trotter, J. *Tetrahedron* **1983**, *39*, 1865.
(6) Lord, P. A.; Olmstead, M. M.; Balch, A. L. *Inorg. Chem.* **2000**, *39*, 1128.
(7) Balch, A. L.; Mazzanti, M.; Noll, B. C.; Olmstead, M. M. *J. Am. Chem. Soc.* **1994**, *116*, 9114.
(8) Attar, S.; Ozarowski, A.; Van Calcar, P. M.; Winkler, K.; Balch, A. L. *Chem. Commun.* **1997**, 1115.
(9) Attar, S.; Balch, A. L.; Van Calcar, P. M.; Winkler, K. *J. Am. Chem. Soc.* **1997**, *119*, 3317.
(10) Stocker, R.; Yamamoto, Y.; McDonagh, A. F.; Glazer, A. N.; Ames, B. N. *Science* **1987**, *235*, 1043.
(11) Nakagami, T.; Taji, S.; Takahashi, M.; Yamanishi, K. *Microbiol. Immunol.* **1992**, *36*, 381.
(12) Mori, H.; Otake, T.; Morimoto, M.; Ueba, N.; Kunita, N.; Nakagami, T.; Yamasaki, N.; Taji, S. *Jpn. J. Cancer Res.* **1991**, *51*, 755.

10.1021/ja010647z CCC: $20.00 
Published on Web 10/04/2001

**Chart 2**

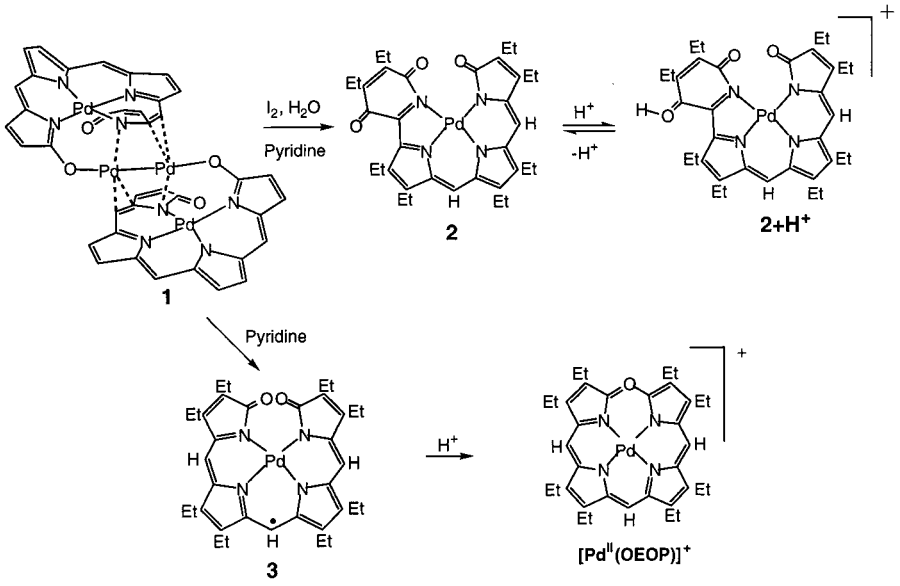


moieties (OEP is the dianion of octaethylporphyrin),[15] coordination of a $[(cymene)Ru]^{2+}$ unit to the face of one pyrrole ring in $Ni^{II}(OEP)$,[16] encapsulation of $Li_4H_4$ units by zirconium meso-octaethylporphyrinogens[17] and **1**, $Pd_4(OEB)_2$ (see Chart 2), in which a $[Pd_2]^{2+}$ unit is bound in $\pi$-fashion to olefinic sites that are exocyclic to pyrrole rings of the octaethylbilindione ligand.[18] Here we report an unprecedented rearrangement of the framework of the bilindione which occurs as a direct consequence of the $\pi$-coordination of the palladium.

## Results and Discussion

**Chemical Reactivity of $Pd_4(OEB)_2$ and Its Reaction Products.** Chart 2 summarizes the chemical reactions discovered in this study. In the structural drawing of $Pd_4(OEB)_2$, the ethyl groups have been omitted for greater clarity.

Molecular halogens are known to cleave $Pd^I-Pd^I$ bonds.[19,20] Consequently, the reactivity of $Pd_4(OEB)_2$ with diiodine was explored as a means toward chemically cleaving this novel dimer. Treatment of **1**, $Pd_4(OEB)_2$, with an excess of diiodine in moist pyridine solution not only cleaves the $Pd^I-Pd^I$ bond but also causes rearrangement and introduction of an oxygen atom into the bilindione skeleton to form the rearranged complex **2**. Black crystals of **2** and orange crystals of *trans*-$Pd(py)_2I_2$ were obtained in 35 and 60% yield, respectively (based on the amount of $Pd_4(OEB)_2$). In contrast when $Pd_4(OEB)_2$ is treated with pyridine in the absence of both $I_2$ and $H_2O$, black crystals of previously characterized, paramagnetic $Pd^{II}(OEB\bullet)$, **3**, are formed.[6] Figure 1 compares the UV/vis absorption spectra of **2** and of $Pd^{II}(OEB\bullet)$. The absorption spectrum of **2** shows features that resemble those of related linear tetrapyrrole complexes such as $Pd^{II}(OEB\bullet)$,[6] $Zn^{II}(OEBOMe)$, and $Co^{II}(OEBOMe)$.[21] Thus, there is an intense band at 438 nm that corresponds to a porphyrin Soret band and a prominent low energy band at 780 nm.

The $^1H$ NMR spectrum of **2** in chloroform-*d* solution consists of a complex multiplet at 1.14−1.34 ppm due to the methyl protons, another complex multiplet at 2.33−3.05 ppm due to the methylene protons, and only two sharp, equally intense singlets at 6.34 and 7.00 ppm due to the two meso-protons. In contrast, $Pd^{II}(OEB\bullet)$ is paramagnetic and does not produce a detectable $^1H$ NMR spectrum.[6] Rather it shows an EPR spectrum with $g = 2.003$ in toluene solution at room temperature.

Infrared spectroscopic studies have allowed the source of the added oxygen atom in **2** to be identified as water, not dioxygen. The infrared spectrum of **2** prepared under routine conditions displays three carbonyl-stretching frequencies at 1702, 1650, and 1620 $cm^{-1}$. When **2** is prepared in the presence of $^{18}O_2$, there is no change observed in the carbonyl region of the infrared spectrum. However, when a small quantity of $H_2{}^{18}O$ is added to the pyridine solution before **1** is converted into **2**, the infrared spectrum of the product shows a marked diminution of the C=O bands at 1650 and at 1620 $cm^{-1}$ and the presence of a new isotope-shifted, carbonyl band at 1607 $cm^{-1}$.

Acidification of a red-brown solution of **2** with trifluoroacetic acid produces a green solution with the spectrum shown in trace C of Figure 1. Both the Soret-like feature and the low-energy band of **2** have undergone a shift to higher energies. The spectral changes seen here are reversible. When the solution used to obtain trace C of Figure 1 is passed through a bed of potassium carbonate, the resulting solution produces the spectrum shown in trace B of Figure 1. This solution can then be treated with an additional portion of trifluoroacetic acid to produce a solution that gives the spectrum shown in trace C of Figure 1. We attribute the spectrum shown in trace C of Figure 1 to the formation of the protonated complex, $\mathbf{2}+\mathbf{H}^+$. Moreover, we suggest that the newly added oxygen atom of the six-membered ring is the site of protonation. Both **2** and $\mathbf{2}+\mathbf{H}^+$ are exceptionally stable species. Complex **2** has been treated with 12 M sulfuric acid in an attempt to remove the palladium ion from

(13) Fox, H. M.; Vevers, G. *The Nature of Animal Colors*; MacMillan Co.; New York 1960; p 102.
(14) Senge, M. *Angew. Chem., Int. Ed. Engl.* **1996**, *35*, 1923.
(15) Alexander, C. S.; Rettig, S. J.; James, B. R. *Organometallics* **1994**, *13*, 2542.
(16) Dailey, K. K.; Yap, G. P. A.; Rheingold, A. L.; Rauchfuss, T. B. *Angew. Chem., Int. Ed. Engl.* **1996**, *35*, 1833.
(17) Floriani, C.; Solari, E.; Solari, G.; Chiesi-Villa, A.; Rizzoli, C. *Angew. Chem., Int. Ed.* **1998**, *37*, 2245.
(18) Lord, P. A.; Olmstead, M. M.; Balch, A. L. *Angew. Chem., Int. Ed.* **1999**, *38*, 2761.
(19) Boehm, J. R.; Doonan, D. J.; Balch, A. L. *J. Am. Chem. Soc.* **1976**, *98*, 4845.
(20) Hunt, C. T.; Balch, A. L. *Inorg. Chem.* **1982**, *21*, 1641.
(21) Latos-Grażyński, L.; Johnson, J.; Attar, S.; Olmstead, M. M.; Balch, A. L. *Inorg. Chem.* **1998**, *37*, 4493.

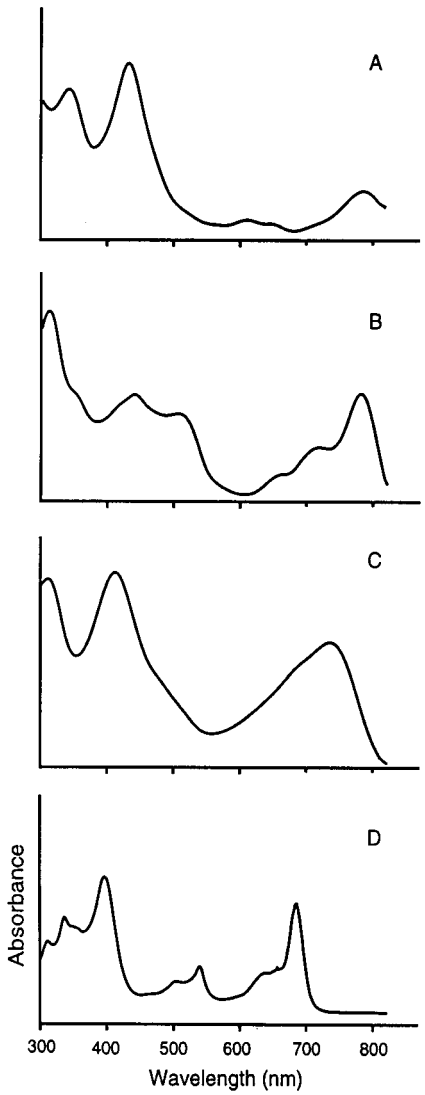


**Figure 1.** The UV/vis spectra of chloroform solutions of A, $Pd^{II}$(OEB•) $\lambda_{max}$ [nm] ($\epsilon$, $M^{-1}$ $cm^{-1}$) = 788 ($1.1 \times 10^4$), 646 ($4.6 \times 10^3$), 608 ($5.1 \times 10^3$), 430 ($3.3 \times 10^4$), 342 ($2.6 \times 10^4$), 284 ($2.4 \times 10^4$); B, the rearranged product **2** $\lambda_{max}$ [nm] ($\epsilon$, $M^{-1}$ $cm^{-1}$) = 780 ($7.4 \times 10^3$), 714 ($4.2 \times 10^3$), 508 ($6.2 \times 10^3$), 438 ($7.1 \times 10^3$), 348 (sh, $6.8 \times 10^3$), 312 ($1.1 \times 10^4$); C, **2**+$\mathbf{H}^+$ (the rearranged product **2** after treatment with trifluoroacetic acid) $\lambda_{max}$ [nm] ($\epsilon$, $M^{-1}$ $cm^{-1}$) = 767 ($1.10 \times 10^4$), 732 ($7.39 \times 10^3$), 416 ($1.28 \times 10^4$), 304 ($1.20 \times 10^4$); and D, [$Pd^{II}$(OEOP)]($CF_3CO_2$), $\lambda_{max}$ [nm] ($\epsilon$, $M^{-1}$ $cm^{-1}$) = 684 ($2.29 \times 10^4$), 648 ($1.04 \times 10^4$), 540 ($1.15 \times 10^4$), 506 ($7.89 \times 10^3$), 396 ($2.62 \times 10^4$), 352 (sh, $2.38 \times 10^4$), 336 ($2.28 \times 10^4$), 310 ($1.72 \times 10^4$), 278 ($1.22 \times 10^4$).

the complex. However, upon neutralization of the acidified complex only unreacted **2** was obtained.

In contrast, addition of trifluoroacetic acid to a solution of $Pd^{II}$(OEB•) results in its conversion into the verdoheme complex, [$Pd^{II}$(OEOP)]($CF_3CO_2$). This salt has been isolated as a deep purple solid. The UV/vis absorption spectrum of [$Pd^{II}$(OEOP)]-($CF_3CO_2$) is shown in trace D of Figure 1. As is characteristic of verdoheme complexes of many metal ions,[22,23] the spectrum of [$Pd^{II}$(OEOP)]($CF_3CO_2$) consists of a sharp, strong, low-energy feature at 690 nm and a Soret-like feature of nearly equal intensity at 400 nm. The $^1$H NMR spectrum of [$Pd^{II}$(OEOP)]($CF_3$-

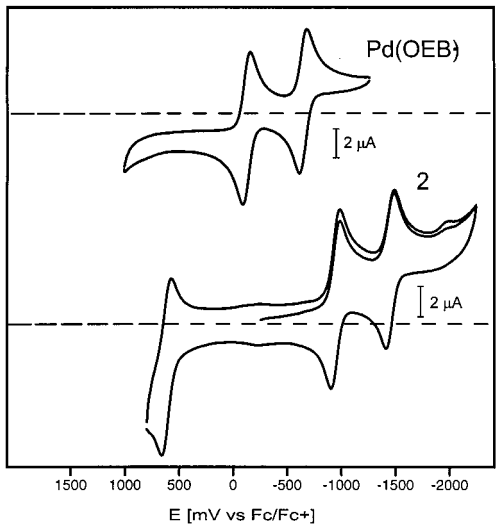


**Figure 2.** Cyclic voltammograms for $Pd^{II}$(OEB•) (top) and the rearranged product **2** (bottom) in dichloromethane solution with 0.10 M tetra(*n*-butyl)ammonium perchlorate as supporting electrolyte and referenced to the ferrocene/ferrocinium couple.

$CO_2$) consists of two meso resonances at 9.60 (two protons) and 9.55 (one proton) ppm, a complex methylene multiplet at 3.79−3.26 ppm, and methyl multiplets at 1.85−1.69 and 1.03−0.83 ppm. Other cases of the cyclization of bilindione complexes to form vedohemes are known as well.[24,25] Note that the rearranged product **2** does not undergo an analogous cyclization. This difference in reactivity originates in the altered nature of **2** with the unusual quinoid ring at the N4 terminus.

Cyclic voltammetry of both **2** and $Pd^{II}$(OEB•) are shown in Figure 2. Each complex is redox active, but $Pd^{II}$(OEB•) is more easily oxidized and more easily reduced than **2**. The cyclic voltammogram of $Pd^{II}$(OEB•) in dichloromethane solution with 0.10 M tetra(*n*-butyl)ammonium perchlorate as the supporting electrolyte shows a reversible oxidation at −167 mV and a reversible reduction at −667 mV, which is consistent with the behavior of other complexes of octaethylbilindione.[6,9] In contrast, **2** undergoes a reversible, one-electron oxidation at 660 mV and two reversible, one-electron reductions at −952 and −1420 mV.

Attempts to form mixed-metal dimers, $Pd^{I}_2M^{II}_2(OEB)_2$, through treatment of $M^{II}$(OEB•) (M = Ni, Co) with palladium-(II) acetate resulted only in the formation of $Pd_4(OEB)_2$ as shown by the $^1$H NMR and mass spectra of the products. Thus, palladium was able to replace the metal originally chelated by the four tetrapyrrole nitrogen atoms as well as to bind to the ligand periphery to form the $\pi$-bonded, dimeric structure.

**The Molecular Structure of the Skeletally Rearranged Product, 2.** The structure of this complex has been determined by X-ray crystallography. A perspective view of the molecule is shown in Figure 3 and selected interatomic distances and angles are given in the figure caption.

The molecule has no crystallographically imposed symmetry. The palladium atom is coordinated by the four nitrogen atoms of the tetrapyrrole ligand. The Pd−N distances span a narrow range (1.997(2)−2.044(2)) and are similar to the Pd−N distances in $Pd^{II}$(OEB•) (2.011(4) and 2.012(4) Å)[6] and in $Pd^{II}$(OEP)

(22) Balch, A. L.; Latos-Grażyński, L.; Noll, B. C.; Olmstead, M. M.; Szterenberg, L.; Safari, N. *J. Am. Chem. Soc.* **1993**, *115*, 1422.

(23) Balch, A. L.; Mazzanti, M.; St. Claire, T. N.; Olmstead, M. M. *Inorg. Chem.* **1995**, *34*, 2194.

(24) Furhop, J.-H.; Salek, A.; Subramanian, J.; Mengersen, C.; Besecke, S. *Liebigs Ann. Chem.* **1975**, 1131.

(25) Koerner, R.; Olmstead, M. M.; Ozarowski, A.; Phillips, S. L.; Van Calcar, P. M.; Winkler, K.; Balch, A. L. *J. Am. Chem. Soc.* **1998**, *120*, 1274.

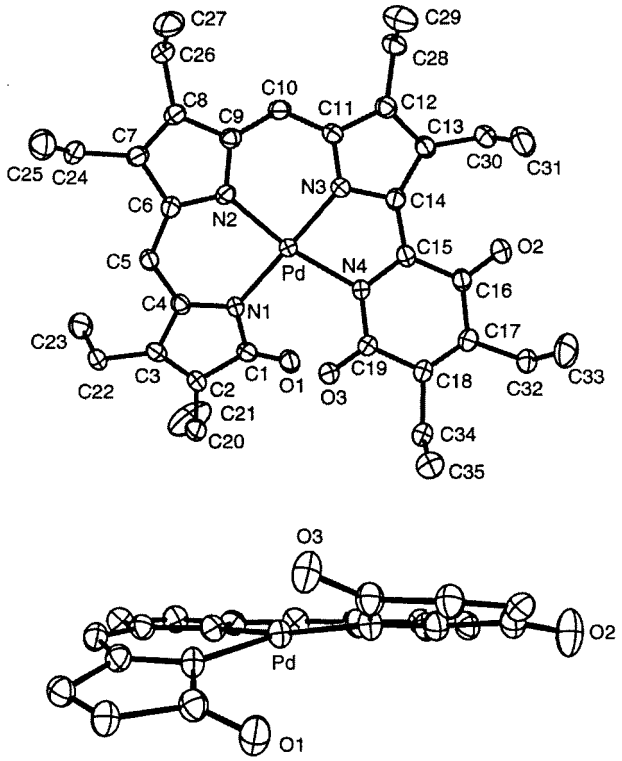


**Figure 3.** (Top) Perspective view of an isolated molecule of the rearranged product **2** with 50% thermal contours. Bond distances (Å): Pd−N(1), 2.015(2); Pd−N(2), 1.997(2), Pd−N(3), 1.942(2), Pd−N(4), 2.044(2), C(1)−O(1), 1.219(3), C(16)−O(2), 1.225(3), C(19)−O(3), 1.220(3). Bond angles (deg): N(1)−Pd−N(2), 89.94(9), N(1)−Pd−N(3), 171.37(10), N(1)−Pd−N(4), 102.28(9), N(2)−Pd−N(3), 90.16(9), N(2)−Pd−N(4), 166.84(9), N(3)−Pd−N(4), 78.51(9). (Bottom) View of **2** which emphasizes the helical nature of the ligand. Ethyl groups have been removed from the lower drawing for clarity.

(2.017, 2.010 Å).[26] As a consequence of the helical nature of the ligand, which allows it to avoid unfavorable contacts at the carbonyl portions, the palladium ion is distorted from the usual planar geometry. This is best seen in the trans N(1)−Pd−N(3) and N(2)−Pd−N(4) angles (171.37(10) and 166.84(9)° respectively) which are compressed from the ideal 180°.

The skeletal rearrangement has led to the formation of a new six-membered ring at the N(4) terminus of the ligand. This six-membered ring is apparently formed by migration of a pyrrole N−C bond from the α-carbon atom of the pyrrole to the adjacent meso carbon atom. Note that this site corresponds to the site of $\pi$-coordination of the $Pd^{I}$ centers in **1**. The former pyrrole α-carbon atom, which is no longer bound to nitrogen, has been converted into a keto function. The C(16)−O(2) distance is 1.225(3) Å. Other distances within the ligand are shown in Figure 4. The noticeable bond length alternations at the N(1) and N(4) termini of the ligand are consistent with bond localization within those parts of the molecule. In contrast the structure of $Pd^{II}$(OEB•) reveals two-fold rotational symmetry and a somewhat greater degree of bond delocalization.[6]

A common supramolecular structural element, a tab/slot interaction between the lactam oxygen of one molecule with a pocket of three C−H hydrogen bond donors, has been found to dominate the solid-state structures of a number of complexes obtained from octaethylbilindione.[6,9] The C−H hydrogen bond donors consist of a meso C−H group and two methylene C−H groups from the adjacent ethyl groups. This tab/slot feature is

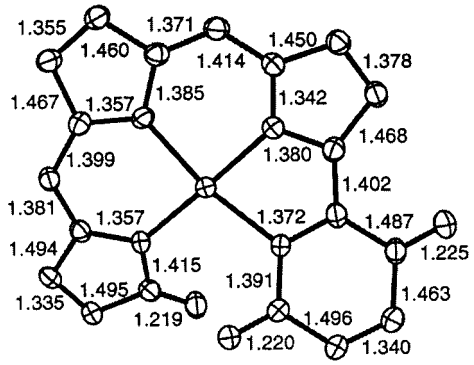


**Figure 4.** A drawing of the rearranged product **2** that shows bond distances within the ligand and emphasizes bond localization at the ends of the molecule. Ethyl groups have been removed for clarity.

also present in the solid-state structure of the rearranged product **2**. Figure 5 shows the interactions between two molecules of **2**. The tab/slot interaction involves the lactam oxygen at the N1 terminus of the ligand. The oxygen atoms at the N4 terminus of the ligand do not participate in such hydrogen bonding. These tab/slot interactions lead to the organization of individual molecules of **2** into chains.

**The Structure of *trans*-Pd(py)$_2$I$_2$.** The molecular structure and solid-state packing of *trans*-Pd(py)$_2$I$_2$ are shown in Figure 6. The palladium atom resides at a crystallographic center of symmetry. The complex consists of a planar *trans*-PdN$_2$I$_2$ unit with the plane of the pyridine ligand making an angle of 76.4° with the plane of the PdN$_2$I$_2$ portion. The molecular dimensions are consistent with those reported for the related complexes *trans*-Pd(py)$_2$Cl$_2$[27] and *trans*-Pd(py)$_2$I$_6$.[28] In the solid the *trans*-Pd(py)$_2$I$_2$ molecules are stacked along the *c* axis. The spacing between palladium centers and between the parallel pyridine rings of adjacent molecules is 5.471 Å. The closest intermolecular contacts are the 3.202 and 3.182 Å separations between iodide ligands and hydrogen atoms of pyridine ligands of neighboring molecules. These distances are at the short end of the expected range (Å) for van der Waals contacts of this type.[29]

## Conclusions

The process that converts Pd$_4$(OEB)$_2$, **1**, to the rearranged product, **2**, is clearly a complex, multistep process that involves cleavage of the Pd−Pd and Pd−C bonds, oxidation of palladium, migration of the nitrogen atom from one carbon to another, and introduction of the oxygen atom via a hydrolytic process, not necessarily in this particular sequence. Nevertheless, it appears that $\pi$-coordination of metal centers to the periphery of tetrapyrroles, and by implication to porphyrins and perhaps phthalocyanines, offers a means for modification of the fundamental backbones of such molecules.

## Experimental Section

**Preparation of Compounds.** Pd$_4$(OEB)$_2$, **1**,[18] and $Pd^{II}$(OEB•), **3**,[6] were prepared as described previously.

**Synthesis of PdC$_{35}$H$_{42}$N$_4$O$_3$, 2.** In air, Pd$_4$(OEB)$_2$ (32 mg, 0.021 mmol) was dissolved in pyridine (15 mL). To this orange-brown solution, I$_2$ (21.3 mg, 0.080 mmol) was added. The resulting green solution was stirred for 3 h. The solvent was evaporated to dryness

(26) Stolzenberg, A. M.; Schussel, L. J.; Summers. J. S.; Foxman, B. M.; Petersen, J. L. *Inorg. Chem.* **1992**, *31*, 1678.

(27) Viossat, P. B.; Dung, N.-H.; Robert, F. *Acta Crystallogr., Sect. C* **1993**, *C49*, 84.

(28) Tebbe, K.-F.; Gräfe-Kavoosian, A.; Freckmann, B. *Z. Naturforsch.* **1996**, *51b*, 999.

(29) Huheey, J. E.; Keiter, E. A.; Keiter, R. L. Inorganic Chemistry. In *Principles of Structure and Reactivity*, 4th ed; Harper Collins New York, 1993; p 292.

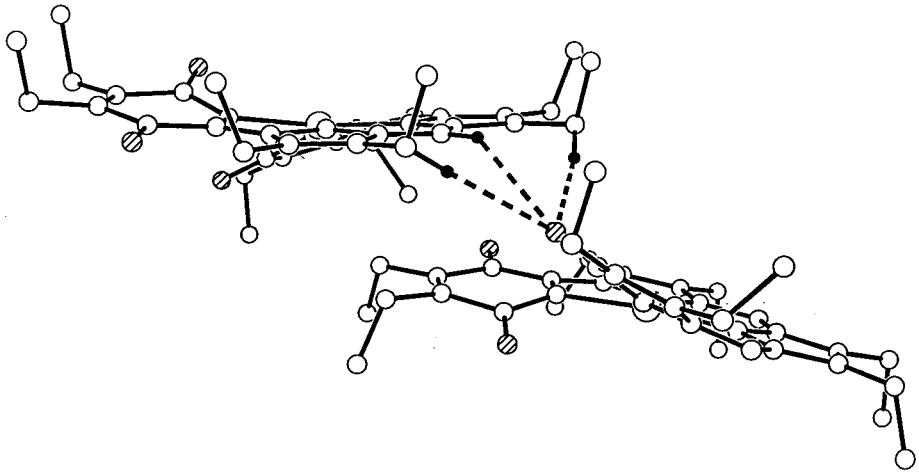

**Figure 5.** A view of two molecules of the rearranged product **2** which shows the tab/slot interactions between the molecules. Oxygen atoms are hatched, and the hydrogen atoms involved in the tab/slot motif are shown as solid circles.

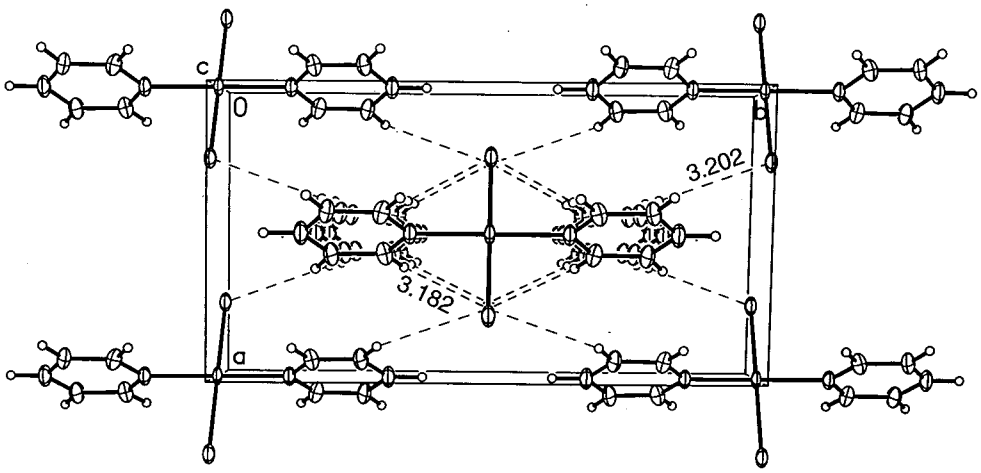


**Figure 6.** Molecular structure and solid-state packing of *trans*-$Pd(py)_2I_2$. Bond distances (Å): Pd−N(1), 2.018(8); Pd−I, 2.6225(15). Bond angles (deg): N(1)−Pd−N(2), I−Pd−I, 180 °, N−Pd−I, 90 °.

under vacuum. The dark residue was taken up in dichloromethane (50 mL). The red-brown dichloromethane solution was washed with water (3 × 100 mL) and dried over solid $Na_2SO_4$. After filtration, the solution was evaporated to dryness. The residue was subject to chromatography on a silica gel column (2 cm × 8 cm) with 1:1 dichloromethane: chloroform mixture as fluent. The first pink and yellow fractions were combined and after recrystallization produced *trans*-$PdI_2(py)_2$ (yield 13.1 mg, 60.3%). The product eluted in the third, red-brown band. This fraction was collected, evaporated to dryness, and vacuum-dried at 115° overnight: yield 9.9 mg, 35%. Black crystals were grown by slow diffusion of pentane into a toluene solution of the compound. $^1$H NMR (300 MHz, $CDCl_3$): $\delta$ (ppm), 6.995 (s, meso-H), 6.334 (s, meso-H), 3.054−2.3247 (m, methylene), 1.327−1.139 (m, methyl). Infrared spectrum (KBr pellet) 2969 s, 2931s, 2872m, 1703s, 1650s, 1621m, 1575m, 1550s, 1533s, 1498m, 1460m, 1390m, 1372m, 1269w, 1230m, 1215s, 1142s, 1092w, 1076s, 1017s, 958w, 928w, 895m, 879m, 813w, 798m, and 788w.

***trans*-$PdI_2(py)_2$.** Orange *trans*-$PdI_2(py)_2$ was obtained from the reaction which produced the rearranged complex, **2**, as described above. Crystals were grown as orange blocks by slow diffusion of ethanol into a dichloromethane solution of *trans*-$PdI_2(py)_2$.

**$[PdC_{35}H_{42}N_4O_3H](CF_3CO_2)$, $[2+H^+](CF_3CO_2)$.** The reaction was monitored using UV/vis spectroscopy. A 1 mL portion of a solution of the rearranged product **2** in dichloromethane was placed in a UV/vis cell, and its UV/vis absorption spectrum was recorded. To this red-brown solution 1 drop of trifluoroacetic acid was added to form a bright green solution. The UV/vis spectrum of the resulting solution is shown in trace C of Figure 1. Then the green solution was filtered through a pad of solid potassium carbonate. The UV/vis absorption spectrum of the red-brown filtrate was identical to that of the original rearranged product, **2**. This process of acidification and neutralization can be repeated several times without decomposition.

**$[Pd^{II}(OEOP)](CF_3CO_2)$.** A sample of $Pd^{II}$(OEB•), **3**, (7.9 mg, 0.012 mmol) was dissolved in dichloromethane (10 mL). To this green solution 1 mL of trifluoroacetic acid was added. The solution was stirred for 5 min. The resulting green solution was passed through a pad of solid potassium carbonate. The filtrate was collected and the solvent evaporated. The residue was dissolved in dichloromethane and subjected to chromatography on silica gel with dichloromethane and increasing amounts of methanol (0, 1, 2, 5, and 10%) as eluant. The product eluted as a purple fraction with 10% methanol in dichloromethane: yield 3.5 mg, 39%. $^1$H NMR (300 MHz, $CDCl_3$): $\delta$ (ppm) 9.601 (s, meso-H), 9.554 (s, meso-H), 3.795−3.262 (m, methylene), 1.846−1.693 and 1.027−0.826 (m, methyl). MALDI mass spectrum (positive ion): parent ion cluster with most intense feature at 641.5 amu and correct isotope distribution pattern.

**Cyclic Voltammetry.** DC-cyclic voltammetry was performed using the BAS CV-50W potentiostat in a three-electrode cell. The working electrode was a gold wire (Bioanalytical system) with a diameter of 1.5 mm. Before each experiment the electrode was polished with fine carborundum paper and a 0.5 $\mu$m alumina slurry in sequence. The electrode was then sonicated to remove the traces of alumina from the surface, washed with water, and dried. A silver wire immersed in 0.01 M $AgNO_3$ and 0.09 M tetra(*n*-butyl)ammonium perchlorate (TBAP) in acetonitrile and separated from the working solution by a ceramic tip (Bioanalytical Systems) served as the reference electrode. Potentials are expressed by reference to the ferrocene/ferrocenium redox system.

The counter electrode was a platinum wire with an area of ~0.1 $cm^2$. Tetra(*n*-butyl)ammonium perchlorate (0.10 *M*) served as the supporting electrode.

**X-ray Data Collection.** The crystals were removed from the glass tubes together with a small amount of mother liquor and immediately coated with a hydrocarbon oil on a microscope slide. Suitable crystals were mounted on glass fibers with silicone grease and placed in the cold stream of the diffractometer. For $PdC_{35}H_{42}N_4O_3$, **2**, data were collected on a Bruker SMART CCD with graphite monochromated Mo Kα radiation. For *trans*-$Pd(py)_2I_2$ the crystal was mounted in the 130 K dinitrogen stream of a Siemens P3 diffractometer equipped with a low-temperature apparatus. Lorentz and polarization corrections were applied. Check reflections were stable throughout data collection. Crystal data are given in Table 1.

**Structure Solution and Refinement.** The structures were solved by direct methods for **2** and Patterson methods for *trans*-$Pd(py)_2I_2$, and refined using all data (based on $F^2$) using the software of SHELX-97. For $PdC_{35}H_{42}N_4O_3$, **2**, a semiempirical method utilizing equivalents was employed to correct for absorption.[30] For *trans*-$Pd(py)_2I_2$ an absorption correction was applied with the program XABS2 which calculates 24 coefficients from a least-squares fit of ($1/A$ vs $\sin^2(q)$) to a cubic equation in $\sin^2(q)$ by minimization of $F_o^2$ and $F_c^2$ differences.[31] Hydrogen atoms were added geometrically and refined with a riding model. All non-hydrogen atoms were refined with anisotropic thermal parameters.

**Acknowledgment.** We thank the National Institutes of Health (Grant GM 26226) for financial support.

(30) Blessing, R. H. *Acta Crystallogr., Sect. A* **1995**, *A51*, 33.
(31) XABS2: An empirical absorption correction program. Parkin, S.; Moezzi, B.; Hope, H. *J. Appl. Crystallogr.* **1995**, *28*, 53.

**Table 1.** Crystallographic Data

| | rearranged product **2** | *trans*-$Pd(py)_2I_2$ |
|---|---|---|
| formula | $C_{35}H_{42}N_4O_3Pd$ | $C_{10}H_{10}I_2N_2Pd$ |
| fw | 673.13 | 518.40 |
| *a*, Å | 13.868(3) | 8.022(3) |
| *b*, Å | 14.966(2) | 15.073(11) |
| *c*, Å | 15.018(2) | 5.471(3) |
| α, deg | 90 | 90 |
| *β*, deg | 92.527(11) | 96.33(4) |
| *γ*, deg | 90 | 90 |
| *V*, Å$^3$ | 3113.9(9) | 657.5(6) |
| *Z* | 4 | 2 |
| crystal system | monoclinic | monoclinic |
| space group | $P2_1/n$ | $C2/m$ |
| *T*, K | 163(2) | 130(2) |
| *λ*, Å | 0.71073 (Mo Kα) | 0.71073 (Mo Kα) |
| *ρ*, Mg/m$^3$ | 1.436 | 2.618 |
| *μ*, mm$^{-1}$ | 0.638 | 6.078 |
| min and max transm | 0.84−0.96 | 0.25−0.58 |
| R1 (obs'd data)[a] | 0.048 | 0.047 |
| wR2 (all data, $F^2$ refinement)[b] | 0.100 | 0.131 |

[a] $R1 = \Sigma||F_o| - |F_c||/\Sigma|F_o|$, observed data ($I > 4\sigma I_o$). [b] $wR2 = [\Sigma[\omega(F_o^2 - F_c^2)^2]/\Sigma[\omega(F_o^2)^2]]^{1/2}$, all data.

**Supporting Information Available:** Details of X-ray crystallographic data collection and structure refinement, tables and atomic coordinates, bond distances and angles, anisotropic thermal parameters, and hydrogen atom positions for **2** and *trans*-$Pd(py)_2I_2$ in CIF format. This information is available free of charge via the Internet at http://pubs.acs.org.

JA010647Z